

Drought-induced changes in the actin cytoskeleton of barley (*Hordeum vulgare* L.) leaves

Katarzyna Śniegowska-Świerk¹ · Ewa Dubas² · Marcin Rapacz¹

Received: 28 November 2014 / Revised: 3 March 2015 / Accepted: 5 March 2015 / Published online: 18 March 2015
© The Author(s) 2015. This article is published with open access at Springerlink.com

Abstract Plants have developed different strategies to adapt to various stress conditions including drought. In the present study the drought-induced changes in the actin filament (AFs) network was studied, for the first time, in two barley cultivars of contrasting drought tolerance level. Detached leaves of drought-tolerant (cv. ‘CAM/B1/CI’) and drought-susceptible (cv. ‘Maresi’) cultivars were dried under controlled conditions. The water relations as well as the transcript accumulation of actin (*ACT11*), actin depolymerization factor (*ADF1*) and dehydrin (*HVA1*) encoding genes were studied using qRT-PCR. Quantitative (the relative fluorescence index; RFI) and qualitative drought-induced changes in AF cytoskeleton were observed following staining with phalloidin. It was noticed that tolerant cultivar was characterized with relative water content decreased during drought treatment which was accompanied by increase in *HVA1* expression together with decrease in *ACT11* and *ADF1* transcripts accumulation induced by drought. In drought-susceptible cultivar the expressions of both *ACT11* and *ADF1* were

slightly lower than those in the control. Drought triggered an extensive AF cytoskeleton reorganization within different types of leaf-blade cells. Remarkable changes in AF configuration and its increased amount (fluorescence intensity) were observed mainly in drought-tolerant cultivar. In addition, drought-induced changes in AFs were closely associated with chloroplasts. Those AFs probably controlled drought-induced intracellular chloroplast positioning in mesophyll. Based on the results obtained in the present study, the possible role of AF rearrangements in drought response is discussed.

Keywords *ACT11* gene · Actin filaments (AFs) · Drought · *Hordeum vulgare* · Quantitative polymerase chain reaction

Abbreviations

ACT	Actin
<i>ACT11</i>	Actin gene
<i>ADF1</i>	Actin depolymerization factor gene
ADP	ADP-ribosylation factor 1
CAFs	Cortical actin filaments
CLSM	Confocal laser scanning microscopy
Ct	Cycle threshold; the mean number of cycles required for the fluorescent signal to cross the threshold
CV	Coefficient of variation (calculated in qBase)
DW	Dry weight
EAfs	Endoplasmic actin filaments
EC	Epidermis
FW	Fresh weight
GA	Glutaraldehyde
<i>HVA1</i>	<i>H. vulgare</i> aleurone 1 gene
<i>LEA</i>	Late embryogenesis abundant gene

Communicated by R. Aroca.

Electronic supplementary material The online version of this article (doi:10.1007/s11738-015-1820-0) contains supplementary material, which is available to authorized users.

✉ Katarzyna Śniegowska-Świerk
katarzyna.sniegowska@gmail.com;
k.sniegowska@ur.krakow.pl

¹ Department of Plant Physiology, University of Agriculture in Krakow, Podłużna 3, 30-239 Kraków, Poland

² The Francisek Górski Institute of Plant Physiology, Polish Academy of Sciences, Niezapominajek 21, 30-239 Kraków, Poland

MCs	Mesophyll cells
MES	Actin stabilizing buffer
MTSB	Microtubule stabilizing buffer
MWC	Maximum water capacity
RFI	The relative fluorescence index
RT	Room temperature
TW	Turgid weight
PFA	Paraformaldehyde
qPCR	Real-time quantitative polymerase chain reaction

Introduction

Plants are constantly exposed to different stresses under field conditions. Globally, drought stress (soil and/or atmospheric water deficit accompanied by heat and radiation) greatly disturbs plant growth and survival, seriously limiting crop productivity (Chinnusamy et al. 2004). Water deficit induces a set of morphological, anatomical, physiological, biochemical, and molecular plant responses (Rizhsky et al. 2002; Bartels and Sunkar 2005).

Plants have developed several strategies to control water content through various cellular activities (review in Chaves et al. 2003). It seems that changes in the organization and dynamics of cytoskeleton (Wasteneys and Galway 2003) associated gene expression are the most prominent in cell protection from damage (Kawaguchi et al. 2003; Wasteneys and Yang 2004).

The cytoskeleton is a highly dynamic component of a plant cell, comprising mainly microtubules (MTs) and actin filaments (AFs). Numerous functions of dynamic cytoskeletal networks, important for intracellular activity, have been discerned, namely cell division, cell movement, morphogenesis, and signal transduction. AFs perform many tasks, ranging from cytoplasmic streaming and organelle orientation to the formation of cytoplasmic structure (Staiger and Schliwa 1987). Plant tissues undergoing division contain large amounts of AFs in the phragmoplast (Baluška and Barlow 1993). Since water deficit results in reduced rate of cell division and cell elongation (Meyer and Boyer 1972), this parameter regulates cell shape and volume (Komis et al. 2002), and expression of various genes, e.g. actin (*ACT11*), actin depolymerization factor (*ADF1*) (Liu et al. 2003) and *Hordeum vulgare* aleurone 1 (*HVA1*) genes (Qian et al. 2007).

HVA1 gene is a member of late embryogenesis-abundant (LEA) group 3 protein investigated in barley (*H. vulgare* ssp. *vulgare*), associated with tolerance to water deficit (Wójcik-Jagła et al. 2012). *HVA1* encodes a dehydrin that is important in maintaining proper functioning of plant cells under drought stress.

ADF1 is probably important for actin-based morphological cell plasticity processes in neurons, spines, and synapses (Fischer et al. 1998) and regulation of ion channels by actin filaments (Johnson and Byerly 1993; Rosenmund and Westbrook 1993). Homologues of this gene were described in many plant species, including wheat (Ouellet et al. 2001), rice (Liu et al. 2003) and barley (*HvADF*) (Liu et al. 2003).

Barley (*H. vulgare* L.) could be used as an excellent experimental model addressing drought stresses encountered by crops in the field conditions (Rapacz et al. 2010; Wójcik-Jagła et al. 2012). As barley is an agronomically important species, its genome and physiological response to various stress conditions have been quite well characterized. Nevertheless, there is still insufficient knowledge on the molecular—to physiological mechanism underlying drought stress responses. Therefore, modern techniques such as real time quantitative polymerase chain reaction (qPCR) and confocal laser scanning microscopy (CLSM) could help to provide a detailed insight into the regulatory networks that link the defence against drought stress on the physiological, cellular, and molecular level.

Moreover, it was earlier reported by our group that water deficit causes the induction of *HVA1* gene expression in barley leaves, independently of the root ABA signal (Wójcik-Jagła et al. 2012). According to Wójcik-Jagła et al. (2012) the level of the expression of *HVA1* gene is related to the drought tolerance of barley cultivars but only when the water deficit of the leaves is similar. This suggests some differences in the perception and transduction effectiveness of water deficit in plant cells that can lead to diverse gene expression profile for different genotypes. However, this mechanism needs further research.

We hypothesized that drought treatment induces the changes in AF reorientation and this reorientation may be connected with the differences in drought tolerance observed between two barley cultivars, and water deficit-induced *HVA1* expression profiles. There is little evidence, that the actin cytoskeleton reorganization in the responding types of leaf cells might be a consequence of altered *ACT11* gene expression and participates in responses to stress. Finally, we demonstrate that an immediate increase in *ACT11* mRNA levels and AFs fluorescence abundance is a component of resistance to drought.

Materials and methods

Donor plants and growth conditions

Two barley (*H. vulgare* L.) cultivars: ‘CAM/B1/CI’ and ‘Maresi’ were used in the study. They were chosen on the basis of preliminary results (Filek et al. 2014).

The choice of cv. 'CAM/B1/CI' was based on the significant difference in its drought stress response as compared to cv. 'Maresi'.

The plants were grown in pots filled with a mixture of clay and sand (7:2, v/v) under greenhouse conditions at 25/17 °C (day/night) at 16/8 h (day/night) regime, air humidity 25–60 % and additional light (Philips SON-T lamps). The analyses were performed in the forth leaf stage, (about 4 weeks after sowing).

Water relations

The relative water content (RWC) was measured in the youngest expanded leaf excised from the 4-week old seedling.

Leaves were detached before dawn, weighted fresh (FW) and placed in distilled water in the dark for 24 h to saturate. The following morning, full turgid weight (FTW) was estimated, then leaves were dried at 65 °C for 48 h and dry weight (DW) was determined. RWC was calculated according to Barrs (1968) formula:

$$\text{RWC} = (\text{FW} - \text{DW}) \times (\text{FTW} - \text{DW})^{-1} \times 100\%.$$

qPCR

Gene expression level was measured in the 2nd youngest and fully expanded leaf detached from the 4-week-old seedling. Then the leaves were dried at 35 °C (air drying chamber; Lumel, Zielona Góra, Poland) in darkness for 55, 110, 165, 220 or 275 min.

Accumulation of *ACT11*, *ADF1* and *HVA1* transcripts was analyzed according to the protocol of Rapacz et al. (2010) with substantial modifications. Barley sequences were found in GenBank: actin (*ACT11*)-GenBank ID: AY145451, late embryogenesis abundant protein (*HVA1*)-GenBank ID: FJ026804.1, ADP-ribosylation factor 1-like protein (*ADP*)-GenBank ID: AJ508228.2, actin depolymerization factor (*ADF1*)-GenBank ID: AK370859.1. To select the sequences of primers and probes, Primer Express 3.0 software (Applied Biosystems) was used (Table 1).

RNA isolation was performed with a RNeasy Plant Mini Kit (Qiagen, Hilden, Germany). Isolated RNA was used as the template for reverse transcription combined with the removal of genomic DNA contamination (Quantitect Reverse Transcription Kit, Qiagen, Germany). The quality and concentration of received cDNA were determined spectrophotometrically (Ultrospec 2100 Pro with an ultramicrovolume cell, Amersham Biosciences, Buckinghamshire, UK).

Each PCR reaction was performed in 96-well plates, using a 7500 real-time PCR System (Applied Biosystems,

Foster City, CA, USA) with default cycling parameters (denaturation at 95 °C for 10 min, followed by 40 cycles of incubation at 95 °C for 15 s and 60 °C for 1 min). The reaction volume was 25 µl with 900 nm of each primer, 250 nm of the probe, 2.5 µl of cDNA (c. 38 ng), 12.5 µl of TaqMan Universal PCR Master Mix, and 2.5 µl of RNase-free water.

Real-time PCR with TaqMan-MGB probes was used as the relative quantification method for the detection of the amplification products, with ADP-ribosylation factor 1 (*ADP*) gene as the internal standard according to Rapacz et al. (2012). The number of mRNA copies for each cultivar was calculated as a value relative to control using $\Delta\Delta C_t$ method (Livak and Schmittgen 2001). Due to very low level of *HVA1* transcript in the control samples, the controls (separate for each cultivar) in the analysis of *HVA1* transcript was the number of mRNA copies after 55 min of drying.

Actin protein accumulation

Leaf fragments were frozen and ground to a fine powder in liquid nitrogen. Total leaf proteins were precipitated with isolation buffer (100 mM tricine, 3 mM $\text{MgSO}_4 \cdot 7\text{H}_2\text{O}$, 3 mM EGTA, 1 mM DTT, pH 8.0) dissolved in water (500 µL for 0.03 g of tissue powder), and centrifuged (7 min, 5000 rpm). Proteins were separated by SDS-PAGE using the buffer system of Laemmli (1970). Samples were brought to a concentration of 20 mg ml⁻¹, then mixed with a loading buffer (4 % w/v SDS, 10 M urea, 12 % w/v glycerol, 2 % v/v β-mercaptoethanol, 0.01 % w/v bromophenol blue in 50 mM Tris, pH 6.8) in the volume ratio 1:1, incubated in 95 °C for 7 min, and loaded into a 10 % polyacrylamide gel with a 4 % stacking gel. Together with samples, molecular weight markers (Amresco) were loaded into the gel. Electrophoresis was run in Mini-Protein 3 apparatus (Bio-Rad, USA) as follows: 100 V, 60 min. Polypeptides from freshly electrophoresed gels were transferred (to a polyvinylidenedifluoride membrane (ImmunBlot PVDF; 0.2 mm pore size; Amresco) using a transfer apparatus according to the manufacturer's protocols (Semi-Dry Electrophoretic Transfer Cell, Bio-Rad). After overnight incubation with 2 % nonfat milk in TBST (10 mM Tris, pH 8.0, 150 mM NaCl, 0.5 % Tween 20, pH 8.0), the membrane was washed with TBST and incubated with primary antibody anti-actin (1:2000, Sigma) at 4 °C for 1.5 h. Membrane was washed with TBST three times for 10 min and incubated for 2 h with a 1:2000 dilution of anti-mouse IgG (Sigma) antibody conjugated with alkaline phosphatase. Blot was washed with TBST three times and the complexes were visualized using SIGMAFAST BCIP/NBT alkaline phosphatase activity detection kit. After staining, membranes were photographed with the

Table 1 Sequences of primers and probes used in qPCR experiment

Gene	Forward primer sequence	Reverse primer sequence	Probe sequence
<i>ACT11</i>	CGACAATGGAACCGGAATG	CCCTTGGCGCATCATCTC	FAM-TCAAGGCTGGTTTCG-MGB
<i>HVA1</i>	CGCCCAGGGCAAGGA	TCTCGGCGGCTTCTG	FAM-CCGCCTCCGTCTTCT-MGB
<i>ADP</i>	CGATGAATGCGGCTGAAAT	CCGCTGGCGCAGAGAGT	FAM-ACTGACAAGCTTGGCC-MGB
<i>ADF1</i>	GCAAACAGCAGGGACATTTGA	CTTGGGATAAATGCCGTGTGT	FAM-TAAGGATTGCCCTGAAAG-MGB
<i>SRG6</i>	AATCGACCAGAACAGCTGTCATT	TTGCTTTTCAGCACGTATTGCT	FAM-TGAGACAAGCTGAACGAG-MGB
<i>RPG4</i>	TCGGCGACCTTTCATCAGAT	TGGGATGCACGATGACATG	FAM-TAACCAACCAATTACACCAACA-MGB

ChemiDoc MP gel documentation system (Bio-Rad Laboratories, Inc).

Immunolocalization of actin filaments

The protocol for the whole mount labeling was adapted from Dubas et al. (2012, 2013) with substantial modifications that improved preservation of actin and penetration of Alexa Fluor-phalloidin expressing high affinity to F-actin.

The leaf cuttings were immediately placed in an Eppendorf tube, with 100 μ M actin stabilizing buffer: MES (3-maleimidobenzoic acid *N*-hydroxysuccinimide ester, Sigma) in methanol (MeOH). Then the samples were prefixed in a mixture containing 1 % paraformaldehyde (PFA, SIGMA 76240) and 0.025 % glutaraldehyde (GA, Sigma) in microtubule stabilizing buffer [MTSB: 50 mM 1.4-piperazinediethane sulfonic acid (PIPES, Sigma), 5 mM EGTA (Sigma), 5 mM MgSO_4 , pH 7.0, adjusted with 5 M KOH]. The fixative was removed from the Eppendorf tubes after 10 min and the samples were re-dipped in MTSB with 3 % PFA and 0.025 % GA for 30 min at room temperature (RT). Next, the samples were washed with MTSB with 0.025 % Triton X-100 for 10 min, then treated with a 0.05-M NH_4Cl and 0.05 M NaBH_4 for 5 min, and washed again. To make cell walls permeable to antibodies, they were partly digested in a mixture of 1 % cellulase ('Ozonuka R-10' from *Trichoderma viride*, Serva), 0.8 % pectinase (from *Rhizopus*, Sigma), 0.02 % pectolyase (from *Aspergillus japonicus*, Sigma), and 0.3 % macerozyme (R-10 from *Rhizopus lyophil*, Serva) in MTSB for 30 min at 37 °C. After that the cells were washed 5 times, 10 min each, with MTSB/0.025 % Triton X-100. To enhance cell wall and cell membrane permeability, the material was incubated in MTSB with 10 % DMSO and 3 % Nonidet P-40 for 50 min at RT. After rinsing, a blocking step was performed with 2 % BSA in MTSB at 30 °C.

Alexa Fluor 488-phalloidin (Invitrogen/Molecular Probes A12379), dilution 1:40, was applied overnight in MTSB with 3 % BSA at RT (vacuum). Thereafter, the material was washed 6 times for 10 min with MTSB/0.025 % Triton/0.02 % NaN_3 and 6 times for 10 min with

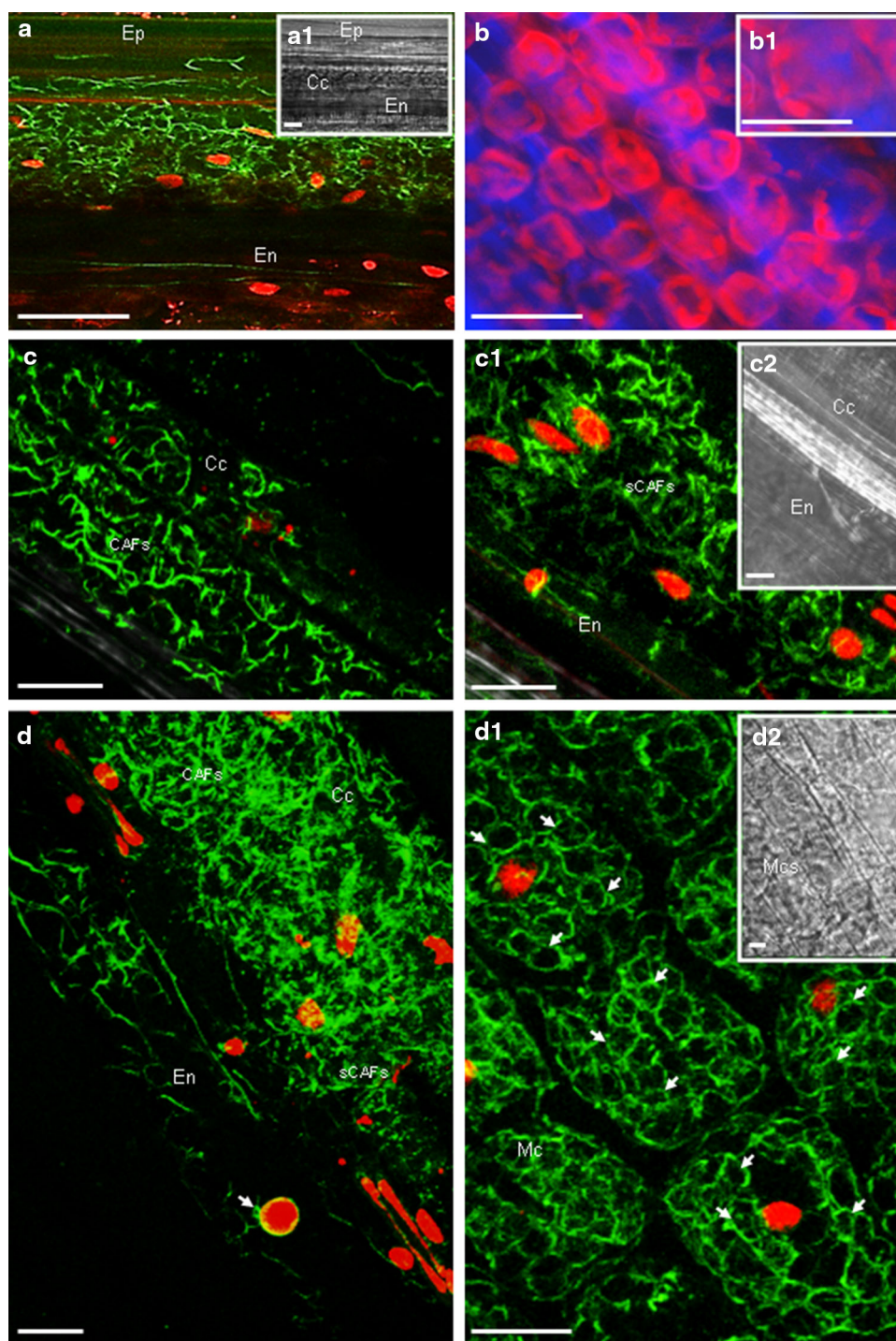
MQ water. The samples were stored in PBS containing 0.02 % NaN_3 . Alexa Fluor-phalloidin saturated the binding sites on AFs what resulted in a specific fluorescent signal. For DNA counterstaining the samples were incubated in 0.1 % propidium iodide (PI, Sigma) for 15 min, washed in PBS, and embedded on slides in Citifluor-glycerol (Citifluor Ltd. in glycerol, AF2, Enfield Cloisters).

Microscopy imaging

Fluorescence microscopy

A strong fluorescence signal from chlorophyll allows observing chloroplasts lying below the epidermis cell layer in the relatively thick leaf sections. Images of chlorophyll autofluorescence were taken using a fluorescent microscope ECLIPSE-E 600 (Nikon). Analysis was performed under filters EX 330-380/DM 400 BA/420.

Fig. 1 Actin filaments and chloroplasts in leaf blade fragments of barley (*H. vulgare* L.) cv. 'CAM/B1/CI'. **a–d** Control leaves with stem endoderm (En), cortical leaf cells (Cc), and epidermis (Ep). Autofluorescence of chloroplasts and cell walls (**b**). Insert on the right shows, in a magnification, a corresponding fragment of image **b** (**b1**). The epidermis in interphase with cortical (CAFs) and subcortical (sCAFs) actin filaments in various configurations: longitudinal, transversal or random to the long cell axis (**a**, **c–c1**, **d**). Insert on the right shows a corresponding transmission image (**c2**). Merged images after Z-series projection (**a**, insert **a1**, **c–c1**, insert **c2**). Endoplasmic actin filaments (EAFs) associate with cytoplasmic strands surrounding the nucleus and form a cage of AFs in the perinuclear cytoplasm (an arrow, **d**). The mesophyll cells (Mcs) with nicely labeled CAFs, sCAFs (arrows) and EAFs (**d–d1**). Prominent and thick AF assemblies encircle centripetally arranged chloroplasts, forming a basket-like structure. Insert on the right shows a corresponding transmission image (**d2**). Merged images after Z-series projection (**a**, **c–c1**, **d–d1**, inserts **a1**, **c2**, **d2**). Visible chloroplasts in transmission light (insert **d2**). **c–c1**, **d–d1** Corresponding images are presenting different focal planes of the same area in the same object. **a**, **c**, **d** Confocal microscopy images of epidermis (Ep) and mesophyll (Mc) cells. Actin filaments were stained with Alexa Fluor 488 phalloidin (green). Nuclei stained with propidium iodide (PI, red). **b** Autofluorescence of chloroplasts (red) in mesophyll and cell walls in epidermis (blue) under UV light. Scale bar 20 μ m

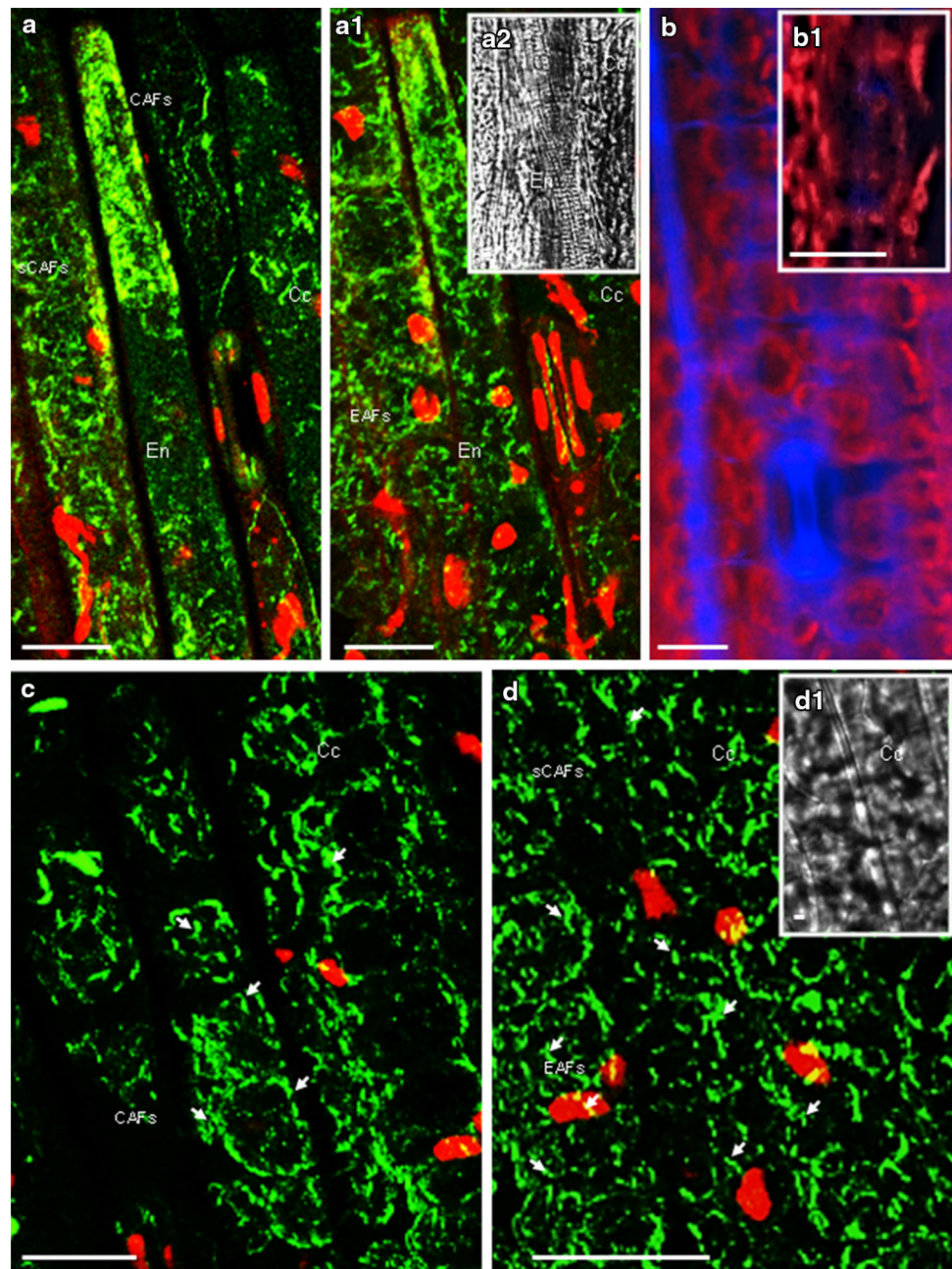


Confocal laser scanning microscopy

Microscopic observations were performed under of C1 confocal laser scanning microscope (CLSM) and fluorescent microscope ECLIPSE-E 600 (Nikon). CLSM images were collected by averaging of 4 full scans. Three-

dimensional images and z-projections of the cells were obtained by collecting series of approximately 10–30 optical sections in the Z-axis, each Section 0.5–1 μm thick. Fluorescence image stacks were registered in parallel in the 488-nm (green) and 561-nm (red) channels. The series of DIC images were registered in a subsequent scan. The

Fig. 2 Actin filaments and chloroplasts in leaf blade fragments of barley (*H. vulgare* L.) cv. 'Maresi'. **a–d** Control leaves with stem endoderm (En) and cortical leaf cells (Cc). Autofluorescence of chloroplasts and cell walls (**b**). Insert on the right shows, in a magnification, a corresponding fragment of image **b** (**b1**). The epidermis (Ep) in interphase with cortical (CAFs, **a**), subcortical (sCAFs, **a**), and endoplasmic (EAFs, **a1**) actin filaments (AFs) in various configurations: longitudinal, transversal or random to the cell long axis. The mesophyll cells (Mc) with nicely labeled AFs in the cortical (CAFs, arrows on **c**), subcortical (sCAFs), and endoplasmic (EAFs, arrows on **d**) cytoplasm (**c**, **d**). Prominent and thick AF assemblies encircle centripetally arranged chloroplasts, forming a basket-like structure (**c**, **d**). Inserts on the right show a corresponding transmission image (**a2**, **d1**). Merged images after Z-series projection (**a–a1**, **c**, **d**, inserts **a2**, **d1**). **a–a1** corresponding images are presenting different focal planes of the same area in the same object. **a–a1**, **c**, **d** Confocal microscopy images of epidermis (Ep) and mesophyll (Mc) cells. Actin filaments were stained with Alexa Fluor 488 phalloidin (green). Nuclei stained with propidium iodide (PI, red). **b–b1** Autofluorescence of chloroplasts (red) in mesophyll and cell walls in epidermis (blue) under UV light. Scale bar 20 μ m



images were acquired and processed using appropriate software, including Imaging system C1, NIS-Elements (AR 2.10 Laboratory Imaging System, Ltd.) and CorelPhoto Paint X5. To estimate the average relative fluorescence intensity (RFI), gray levels across normalized areas (6–8) of subsequent leaf regions (arbitrary units) were quantified using the base package of ImageJ software. Values displayed are the mean of three biological replicates.

Statistical analysis

The data presented for the RWC parameter are means from five replicates (measurements were performed on the

leaves detached from the control plants and from the plants after drought stress procedure).

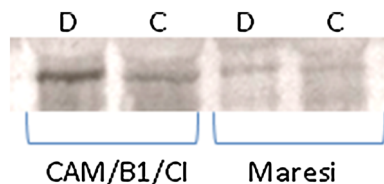
The data presented for gene expression in leaves are means from three replicates (leaves detached from the control plants and from the plants after drought stress at subsequent time points of drying procedure). The data evaluation started with a descriptive statistical analysis (mean \pm SE). ANOVA/MANOVA was performed for assessing the effects of various treatments. Data comparison was based on Tukey's HSD test ($P < 0.05$). All statistical analyses were carried out using STATISTICA 10.0 (StatSoft, Tulsa, OK) software package.

Table 2 RFI across normalized areas (6–8; arbitral units) of subsequent leaf regions

Cultivar	Treatment	Cell type	RFI	
			Mean	Std. error
CAM/B1/CI	Control	Cortical cells (Cc)	49.6	1.72
		Endoderm (En)	13.3	1.33
		Mesophyll (Mc)	44.5	3.11
	Drought	Cortical cells (Cc)	19.9*	2.35
		Endoderm (En)	33.5*	4.63
		Mesophyll (Mc)	13.4*	0.74
Maresi	Control	Cortical cells (Cc)	20.7	2.78
		Endoderm (En)	34.5	1.38
		Mesophyll (Mc)	18.3	3.76
	Drought	Cortical cells (Cc)	16.9	3.12
		Endoderm (En)	31.5	1.27
		Mesophyll (Mc)	24.2	1.67

Values displayed are the mean of three biological replicates

* Values that are significantly different from control values ($P < 0.05$, ANOVA followed by Tukey's HSD test). RFI of epidermis (Ep) not analyzed due to uneven distribution of AF in drought-treated Ep

**Fig. 3** Western blots of actin protein accumulation in barley leaves under control (C) and drought (D) conditions

Results

AFs organization before drought

In both studied genotypes, control leaf epidermis (Ep) displayed various configurations of cortical AFs (CAFs) in interphase: random, longitudinal or transversal to the long cell axis. On the basis of genotype, CAFs configuration differed (Figs. 1a–d, 2a–a1). CAFs formed thick actin bundles, or organized in network of fine AFs or sparsely arranged AF bundles in epidermis (Figs. 1a–a1, 2a). Longitudinal and thick AF bundles were thinner relative to transversely or randomly oriented. These latter AFs lined close to each other by what formed a net-like structure (Figs. 1c, d, 2a). An actin cytoskeleton composed of longitudinal AFs was also found in leaf stem endoderm in cv. 'CAM/B1/CI' (Fig. 1a–a1). In most cortical leaf cells, prominent subcortical (subCAFs) and endoplasmic AFs (EAFs) were also observed (Figs. 1c–c1, 2a1). EAFs were

associated with cytoplasmic strands surrounding the nucleus and formed a cage of AFs in the perinuclear cytoplasm (Fig. 1d).

Control Mcs contained intensely fluorescent AFs in the cortical, subcortical, and endoplasmic cytoplasm (Figs. 1d–d1, 2c, d, On-line resource 1, On-line resource 2). In the cortical cytoplasm, prominent and thick AFs formed assemblies that encircled chloroplasts, forming a basket-like structures (Figs. 1d–d1, 2c). Similarly, in the perinuclear region, F-actin formed curly aggregates randomly oriented around multiple and randomly distributed chloroplasts along the cell walls. Based on the CLSM and fluorescence images, AFs seemed to adhere to the chloroplasts in both, the central and peripheral cytosol (Figs. 1d1, 2d). Special AFs organization in Mc, of both cultivars, coincided with fluorescence intensity presented as RFI. RFI was much higher ($P = 0.001$, Table 2) in CAM/B1/CI, which may suggest a relative higher content of polymerized actin in this cultivar. This suggestion was additionally confirmed by higher accumulation of actin protein (Fig. 3).

AF organization in drought-treated leaf cells

The actin protein accumulation in leaves was higher in drought-tolerant cultivar (Fig. 3). In both cultivars drought induced actin accumulation, especially in drought-tolerant cultivar. The picture is, however, much more complicated when both quantitative (RFI) and qualitative changes in AFs were taken into consideration.

In Ep and Mc cells, the AF cytoskeleton was significantly affected by drought stress. The observed changes differed between cultivars (Figs. 4, 5, On-line resource 3, On-line resource 4). In leaves of drought-tolerant cv. 'CAM/B1/CI', the RFI of AFs in Mc and Cc was significantly weaker in comparison to the control. On the contrary, in En cells, the RFI of AFs stained in drought-treated leaves was very high (Table 2).

Drought-induced changes were observed in AF configuration. In the Ep, the fine CAFs disappeared and numerous cortical, subcortical and endoplasmic AFs arranged in thick and well-organized bundles were formed (Figs. 4a, b, 5a, b). Distinct AFs arranged in the thick and mostly longitudinal to the long axis bundles traversed the subcortical cytoplasm. Longitudinal CAFs gave fluorescence especially in endodermal cells of leaf stems. Longitudinal CAF bundles in cortical leaf cells were thicker relative to the transversal strands and they were preferentially localized in the vicinity of the plasmalemma, lining the plasma membrane regions (Figs. 4b, 5b). The EAF bundles were mainly found in the perinuclear cytoplasm of cortical leaf cells (Figs. 4a, b, 5a, b). Sometimes, transversal and short AFs aligned parallel to each other close to plasma membrane. Those AFs remained at the boundaries and they

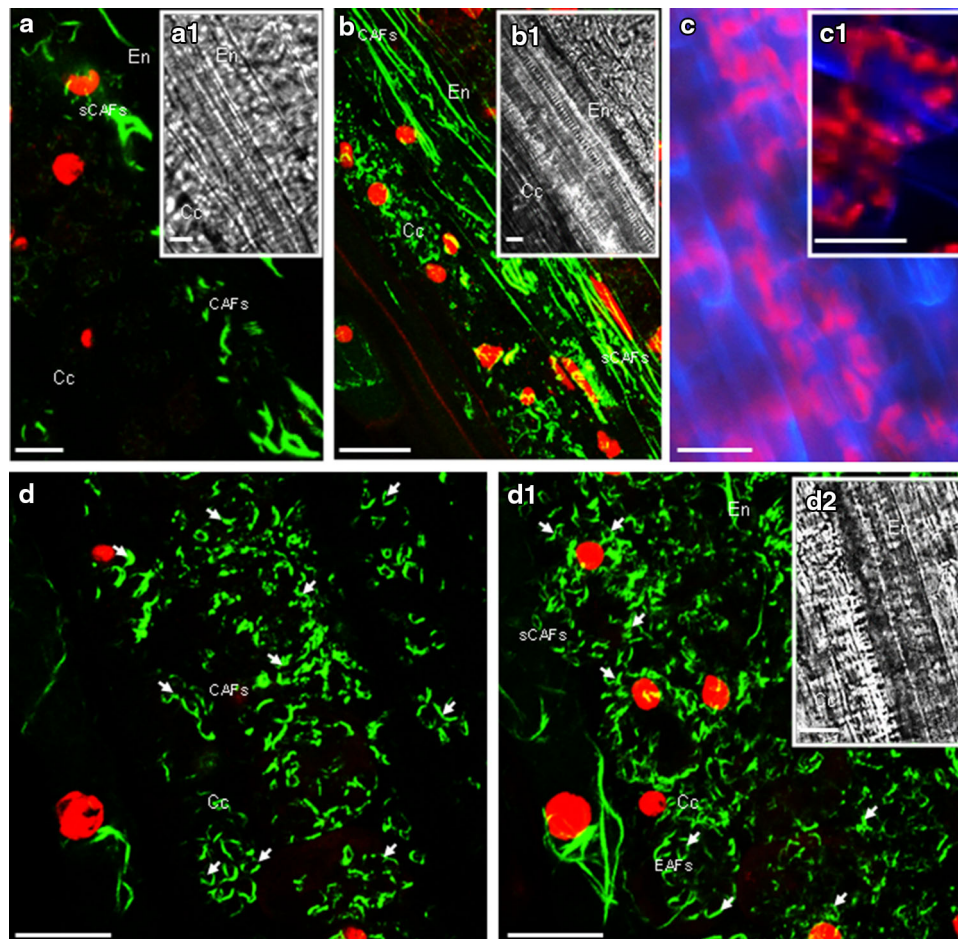


Fig. 4 Actin filaments and chloroplasts in leaf blade fragments of drought-treated barley (*H. vulgare* L.) cv. ‘CAM/B1/CI’. **a–d** Drought-treated leaves with stem endoderm (En) and cortical leaf cells (Cc). Ep (**a–c**) and Mc cells (**c–d**). Short and thick AFs fragments without any orientation in the cortical (CAFs) and subcortical (sAFs) cytoplasm of epidermis cortical cells (**a**). Numerous cortical (CAFs) and subcortical AFs (sAFs) arranged in thick and well-organized bundles longitudinally orientated in endodermal cells of leaf stems and short and thick AF fragments without any orientation in the cortical and subcortical cytoplasm of epidermis cortical cells (**b**, insert **b1**). Autofluorescence of chloroplasts and cell walls (**c**). Insert on the right shows, in a magnification, a corresponding fragment of image **c** (**c1**). AFs in the cortical (CAFs,

arrows on **d**), subcortical (sAFs), and endoplasmic (EAFs, arrows on **d1**) cytoplasm of Mcs (**d–d1**). Fragments of basket-like AF structures (arrows) in the cortical cytoplasm (**d**) and in the perinuclear region of Mc (**d1**, arrows). Inserts on the right show a corresponding transmission image (**a1**, **b1**, **d2**). Merged images after Z-series projection (**a**, **b**, **d**, inserts **a1**, **b1**, **d2**). **d–d1** Corresponding images are presenting different focal planes of the same area in the same object. **a**, **b**, **d–d1** Confocal microscopy images of epidermis (Ep) and mesophyll (Mc) cells. Actin filaments were stained with Alexa Fluor 488 phalloidin (green). Nuclei stained with propidium iodide (PI, red). **c**, **c1** Autofluorescence of chloroplasts (red) in mesophyll and cell walls in epidermis (blue) under UV light. Scale bar 20 μm

appeared to be connected to form a dense network (Fig. 5a).

Mcs contained intensely fluorescent AFs in the cortical, subcortical and endoplasmic cytoplasm (Figs. 4d–d1, 5d, e). In the cortical cytoplasm, the fluorescence of prominent and thick basket-like structure of AFs was reduced (Figs. 4d, 5d). Similarly, curly aggregates of F-actin oriented around chloroplasts were less prominent in the perinuclear region (Figs. 4c–c1, d1–d2, 5c–c1, e–e1). AFs seemed to adhere to the chloroplasts that were dispersed in the peripheral cytosol of MCs (Figs. 4c–c1, 5c–c1). Even though enhanced fluorescence of AFs was found in both

genotypes, a stronger signal came from AFs in MCs of susceptible cv. ‘Maresi’ (Fig. 5d1–d2). Curve-shaped and transverse arcs of AFs of cv. ‘Maresi’ adhered in Mcs to the chloroplasts in their cortical and subcortical cytoplasm (Fig. 5c–e). These AFs seemed to be longer than AFs in ‘Maresi’ control cells (Fig. 2c, d).

ACT11 gene expression

As mentioned before, no changes in actin protein accumulation were observed during drought treatment; however, drought treatment revealed different profiles of

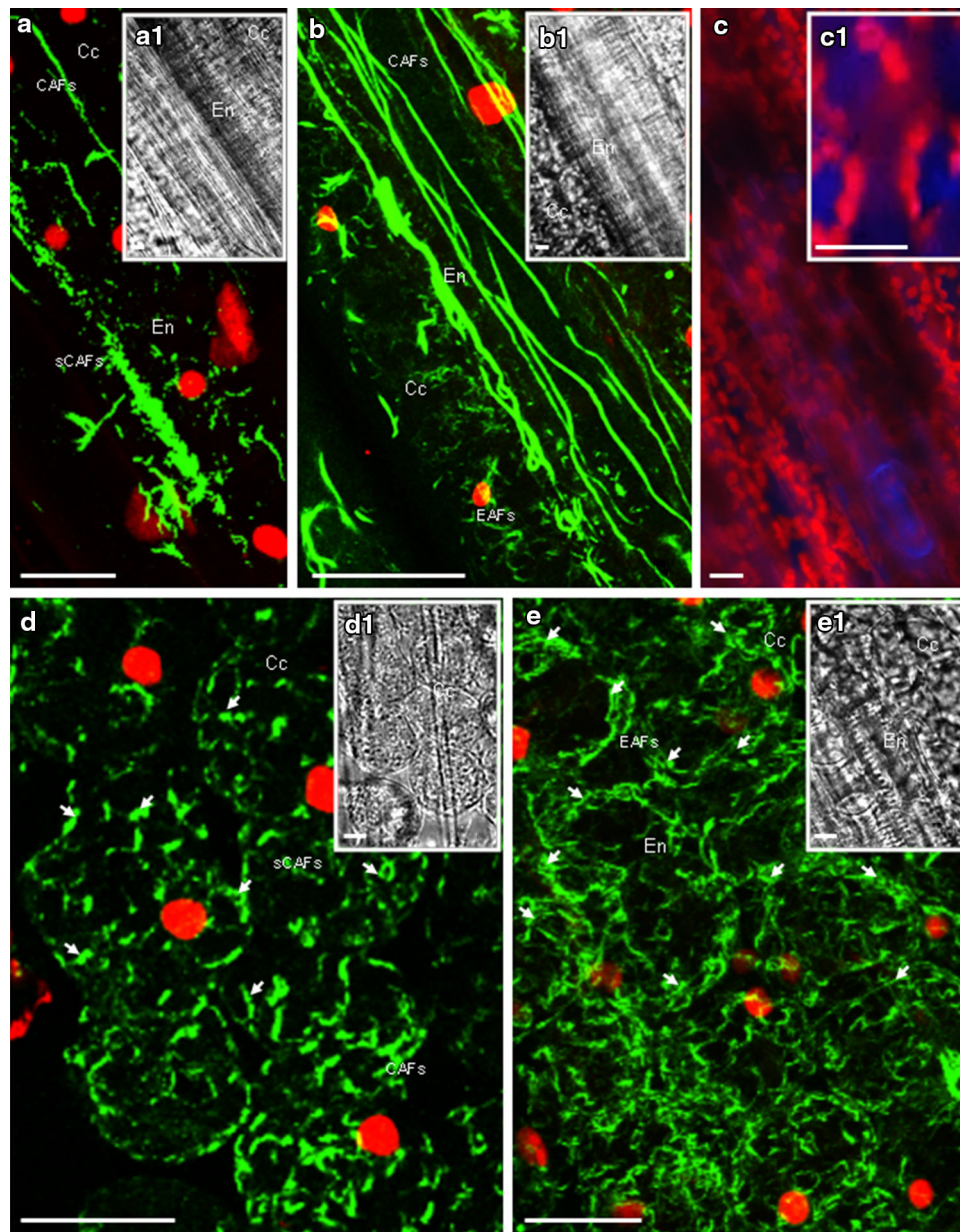


Fig. 5 Actin filaments and chloroplasts in leaf blade fragments of drought-treated barley (*H. vulgare* L.) cv. ‘Maresi’. **a–d** Drought-treated leaves with stem endoderm (En) and cortical leaf cells (Cc). Ep (**a, b**) and Mc cells (**c, d, e**). Numerous cortical (CAFs), subcortical (sAFs) and endoplasmic (EAFs) AFs arranged in thick and well-organized bundles (**a, b**). AFs oriented transversally (**a**) and longitudinally (**b**) in the cortical and subcortical cytoplasm. Both types of AFs line the plasma membrane. Autofluorescence of chloroplasts and cell walls (**c**). Inserts on the *right* shows, in a magnification, a corresponding fragment of image **c** (**c1**). AFs in the cortical (CAFs), subcortical (sAFs, *arrows* on **d**), and endoplasmic

(EAFs, *arrows* on **e**) cytoplasm of Mc, (**d, e**). Fragments of basket-like AF structures in the cortical cytoplasm and in the perinuclear region of Mc. Confocal microscopy image of epidermis (Ep) and mesophyll (Mc) cells—merged images after Z-series projection (**a, b, d, e**). Inserts on the *right* show a corresponding transmission image (**a1, b1, d1, e1**). **a, b, d, e** Confocal microscopy images of epidermis (Ep) and mesophyll (Mc) cells. Actin filaments were stained with Alexa Fluor 488 phalloidin (green). Nuclei stained with propidium iodide (PI, red). **c–c1** Autofluorescence of chloroplasts (red) in mesophyll and cell walls in epidermis (blue) under UV light. Scale bar 20 μm

ACT11 transcript accumulation in drought-tolerant (cv. ‘CAM/B1/CI’) and -susceptible (cv. ‘Maresi’) genotypes (Fig. 6). *ACT11* gene expression level increased in response to drought, but this effect was clearly more

pronounced in cv. ‘Maresi’, where the relative mRNA accumulation was higher than in cv. ‘CAM/B1/CI’ with the exception of the 55th min of drying. *ACT11* transcript accumulation in cv. ‘Maresi’ increased throughout the

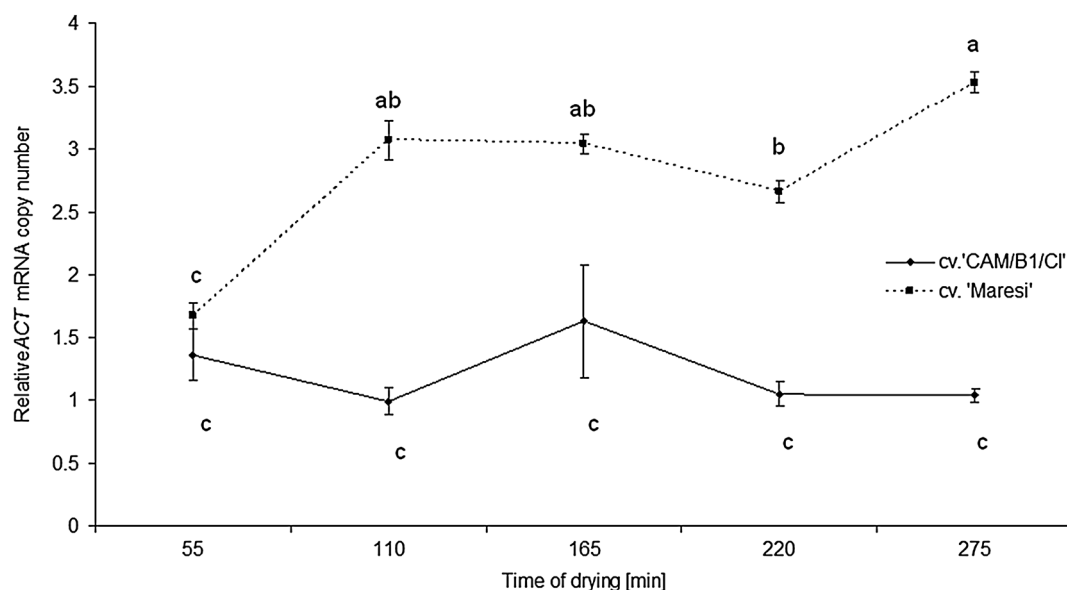


Fig. 6 Relative quantification of the *ACT11* transcript accumulation with well-watered leaves as the control and *ADP* as a reference gene expression profiles during drying of the leaves of drought-tolerant cv.

'CAM/B1/CI' and drought-susceptible cv. 'Maresi' (mean \pm SE). Values marked with the same letters did not differ statistically at $P = 0.05$ according to Tukey's HSD test

Table 3 The effect of 275 min of leaf drying at $+30$ °C on water content (WC), relative water content (RWC) and *HVA1* and *ADF1* transcript accumulation in two barley cultivars

Cultivar	Conditions	WC mean	RWC mean	<i>HVA1</i> (drying) (max/early)	<i>ADF1</i> (drying) (late/early)
CAM/B1/CI	Control	87.05 \pm 0.48a	91.22 \pm 1.04b		
	Drought treatment	83.45 \pm 0.63b	70.19 \pm 1.23c	58.52 \pm 16.62a	0.348 \pm 0.114b
Maresi	Control	89.29 \pm 0.63a	97.86 \pm 0.28a		
	Drought treatment	85.61 \pm 0.83b	68.01 \pm 2.44c	12.61 \pm 1.19b	1.163 \pm 0.071a

HVA1 transcript accumulation relative to the expression in cv. 'Maresi' after 55 min of drying (no expression observed in the control); *ADF1* transcript accumulation relative to the control; *ADP* was a reference gene. Mean \pm SE. Homogeneity groups (Tukey's HSD test, $P = 0.05$) within the parameter are marked with letters

entire drying phase. The level of transcript accumulation in cv. 'CAM/B1/CI' was constant and close to the control level.

The effect of drought treatment on *ADF1* and *HVA1* expression level and leaf water relations

The drought treatment used in the present experiment affects water relations in leaves and trigger a molecular response increasing the expression of either *ADF1* and *HVA1* gene (Table 3). *ADF1* transcript accumulation decreased during drying in more drought-tolerant cv. 'CAM/B1/CI', whereas remains stable in cv. 'Maresi'. The increase in the expression of dehydrin-encoding *HVA1* gene was higher in cv. 'CAM/B1/CI' than in cv. 'Maresi'. In cv. 'CAM/B1/CI' the lower decrease in RWC was also observed during drying. On the other hand lower RWC was observed in cv.

'CAM/B1/CI' before drought. Decrease in water content (WC) was similar in both cultivars (Table 3).

Discussion

Here we provide the first report that changes in plant AF organization occur in response to drought stress in drought-tolerance dependent manner which could be interpret as an adaptation. *H. vulgare* plants activate both common and cultivar-specific mechanisms to avoid water lost and survive the stress conditions. Although significant rearrangements of the actin cytoskeleton in response to different extracellular stimuli are well documented (Staiger 2000), our experiments revealed that the formation of thick bundles of longitudinally arranged AFs in the vicinity of epidermis plasmalemma was caused by water deficit in barley

leaves. AFs assembled beneath the plasma membrane provided mechanical support against water lost. Such pattern of AF configuration resembles the straight ‘stress fibers’ which would easier regulate cell shape and volume in interphase (Komis et al. 2002), thus improving the drought defence. Those AFs might probably assist wall reinforcement by plasma membrane lining in epidermis. As AFs are linked to the plasma membrane via actin-binding proteins (Baluška et al. 2003), actin remodeling ought to be involved in plasma membrane reinforcement.

Our experiments confirmed that drought had a distinct effect on chloroplast and AF reorganization in mesophyll. In the mesophyll of drought-tolerant cv. ‘CAM/B1/CI’ drought-induced chloroplast positioning was limited to the cell periphery and coincided with diminished AF fluorescence in the mesophyll cell center. The lower RFI in comparison with RFI calculated for cv. ‘Maresi’, implies smaller number of actin filaments. Curly aggregates of transverse arcs of AFs in the mesophyll cell center were less prominent in the cortical and perinuclear cytoplasm, as compared to control in both tested cultivars. In cv. ‘Maresi’ AFs surrounded the chloroplasts that were positioned close to the nucleus and in the periphery of the mesophyll cell, whereas in cv. ‘CAM/B1/CI’ AFs surrounded the chloroplasts that were positioned in the cortical cytoplasm, away from the nucleus. Drought induced the AFs in mesophyll tend to organize in a shorter arcs. Interestingly, these curve-shaped AFs of cv. ‘Maresi’ seemed to be longer than those in cv. ‘CAM/B1/CI’. Probably, AF extending occurred by assembly of short actin bundles in that drought-susceptible genotype.

The characteristic circular arrays of transverse AFs may function to maintain the specific distribution pattern of barley chloroplasts. Moreover, the aggregative movement of chloroplasts is known to be actin dependent (Schmidt von Braun and Schleiff 2008). It is thought to be a protective response under stress conditions (Maai et al. 2011). The chloroplast peripheral positioning observed herein is probably due to short cortical AFs around the chloroplasts perimeter but not endocyttoplasmic actin. An actin-based motility system could be deduced by detailed observation of chloroplast movement (Tsuboi and Wada 2011; Yamashita et al. 2011).

Although changes in AFs configuration were genotype-dependent in both Ep and Mc cells, longitudinally and transversally oriented AFs were thicker relative to the same strands in control tissues. Because thicker AFs are likely to be composed of a greater number of individual AFs compared with the thinner bundles, it could be assumed that actin synthesis increased or that the actin depolymerization rate decreased. The general drought-induced increase in AFs may be connected with increased expression of *ACT11* gene, whereas differences between

drought-tolerant and drought-susceptible cultivar seem to depend rather on de-polymerization level. In our experiment we observed drought-induced increase in AF content confirmed by western blot analysis of actin protein. This effect was stronger in drought-tolerant cultivar. On the other hand, the increase in *ACT11* gene expression was stronger in less tolerant ‘Maresi’ cultivar, in which less AFs were observed in drought. The possible reason may be connected with large decrease in *ADF1* expression level observed in drought-tolerant ‘CAM/B1/CI’. The increase in ADF protein accumulation was observed during drought response of rice plants (Liu et al. 2003). Drought-induced increase in ADF synthesis was observed in rice roots, which was suggested as a hypothetical increase in the rate of actin turnover (Yang et al. 2003). It should be emphasized that in our study a decrease in *ADF1* expression was observed in very drought-tolerant Syrian land-race of barley but not in less-tolerant European cultivar in which the level increased not significantly. It may be suggested that increased rate of ADF accumulation may be connected with drought-response of non-tolerant plants, as in the case of rice.

The drought-tolerance mechanisms connected with the AFs changes observed herein may determine an effective leaf answer to dehydration by enhancing the cell wall strength. We suppose also that apart from AFs reorganization, genomic control of actin synthesis is needed for successful cell volume regulation. *ACT11* gene overexpression resulting in dramatic elevation of short AFs in the cortical cytoplasm and long AFs in the subcortical and endocyttoplasmic cytoplasm observed in mesophyll of susceptible cultivar may be suggested to be a feedback effect of problems with proper microfilament arrangement. *ACT11* gene was reported also before as being unstable under drought treatment (Rapacz et al. 2012). This outcome is in agreement with previously published results, showing the involvement of actin in the regulation of drought-response in watermelon roots (Yoshimura et al. 2008). The drought-induced changes in the reorganization of AFs within epidermis and mesophyll is accompanied by the activation of genes involved in the perception of drought stress and in the transmission of the stress signal (Shinozaki and Yamaguchi-Shinozaki 2007). In the present study *HVA1* was highly expressed in the drought-treated leaves of the tolerant cv. ‘CAM/B1/CI’. This finding is consistent with previously published results concluding that *HVA1* up-regulation is correlated with better drought tolerance (Sivamani et al. 2000; Wójcik-Jagła et al. 2012). Plants have developed multiple stress perception and signaling pathways, some of which are specific, but others may cross-talk at various steps (Chinnusamy et al. 2004). Some of them include ABA-dependent and ABA-independent pathways (Shinozaki et al. 2003; Shinozaki and

Yamaguchi-Shinozaki 2007). *HVA1* expression was reported to be highly (but not entirely) ABA-independent under drought stress conditions (Wójcik-Jagła et al. 2012). The fact that *HVA1* showed altered response to drought suggests an intriguing possibility that actin acts independently of ABA as well (Luan 2002). AFs acting as an ‘osmosensor’ in ABA-independent drought response were suggested by Liu and Luan (1998) for the guard cells. Hypotonic conditions disrupted AFs, whereas in hypertonic solution they appeared to be organized into a ‘network’ that was distributed throughout the cell body (Liu and Luan 1998). This observation was in fact confirmed in our study for different leaf tissues.

In the present paper we demonstrate that the actin cytoskeleton reorganization (an immediate increase in *ACT11* mRNA levels, change in *ADF1* expression and AFs fluorescence abundance) in leaf cells seems to be a component of drought response in barley leaves. It is hard to confirm at the present stage if AF rearrangements may be involved in the control of some drought-induced gene expression. It is also possible that observed changes were just coincidental elements of early drought response in barley together with observed changes in *HVA1* expression.

Author Contribution Statement Katarzyna Śniegowska-Świerk: sample preparation, PCR and Western blot analysis, writing the first version of the manuscript; Ewa Dubas: microscopic analysis, image processing; Marcin Rapacz: statistical analysis, general supervision. All co-authors were involved in the manuscript preparation.

Acknowledgments This work was supported by The National Science Centre awarded by decision number DEC-2012/07/N/NZ9/02412.

Conflict of interest The authors declare that they have no conflict of interest.

Open Access This article is distributed under the terms of the Creative Commons Attribution License which permits any use, distribution, and reproduction in any medium, provided the original author(s) and the source are credited.

References

- Baluška F, Barlow PW (1993) The role of the microtubular cytoskeleton in determining nuclear chromatin structure and passage of maize root cells through the cell cycle. *Eur J Cell Biol* 61:160–167
- Baluška F, Šamaj J, Wojtaszek P, Volkmann D, Menzel D (2003) Cytoskeleton-plasma membrane-cell wall continuum in plants. Emerging links revisited. *Plant Physiol* 133(2):482–491. doi:10.1104/pp.103.027250
- Barrs HD (1968) Determination of water deficits in plant tissues. In: Kozłowski TT (ed) *Water deficits and plant growth*, vol 1. Academic Press, New York, pp 235–368
- Bartels D, Sunkar R (2005) Drought and salt tolerance in plants. *Crit Rev Plant Sci* 24:23–58. doi:10.1080/07352680590910410
- Chaves MM, Maroco JP, Pereira JS (2003) Understanding plant responses to drought-from genes to the whole plant. *Funct Plant Biol* 30:239–264. doi:10.1071/FP02076
- Chinnusamy V, Schumaker K, Zhu JK (2004) Molecular genetic perspectives on cross-talk and specificity in abiotic stress signaling in plants. *J Exp Bot* 55:225–236. doi:10.1093/jxb/erh005
- Dubas E, Wedzony M, Custers J, Kieft H, van Lammeren AAM (2012) Gametophytic development of *Brassica napus* pollen in vitro enables examination of cytoskeleton and nuclear movements. *Protoplasma* 249:369–377. doi:10.1007/s00709-011-0287-0
- Dubas E, Custers J, Kieft H, Wędzony M, van Lammeren AAM (2013) Characterization of polarity development through 2- and 3-D imaging during the initial phase of microspore embryogenesis in *Brassica napus* L. *Protoplasma*. doi:10.1007/s00709-013-0530-y
- Filek M, Łabanowska M, Kościelniak J, Biesaga-Kościelniak J, Kurdziel M, Szarejko I, Hartikainen H (2014) Characterization of barley leaf tolerance to drought stress by chlorophyll fluorescence and electron paramagnetic resonance studies. *J Agro Crop Sci*. doi:10.1111/jac.12063
- Fischer M, Kaech S, Knutti D, Matus A (1998) Rapid actin-based plasticity in dendritic spines. *Neuron* 20:847–854. doi:10.1016/S0896-6273(00)80467-5
- Johnson BD, Byerly L (1993) A cytoskeletal mechanism for Ca^{2+} channel metabolic dependence and inactivation by intracellular Ca^{2+} . *Neuron* 10:797–804. doi:10.1016/0896-6273(93)90196-X
- Kawaguchi R, Williams AJ, Bray EA, Bailey-Serres J (2003) Water-deficit-induced translational control in *Nicotiana tabacum*. *Plant Cell Environ* 26:221–229. doi:10.1046/j.1365-3040.2003.00952.x
- Komis G, Apostolakis P, Galatis B (2002) Hyperosmotic stress-induced actin filament reorganization in leaf cells of *Chlorophyton comosum*. *J Exp Bot* 53:1699–1710. doi:10.1093/jxb/erf018
- Laemmli UK (1970) Cleavage of structural proteins during the assembly of the head of bacteriophage T4. *Nature* 227:680–685
- Liu K, Luan S (1998) Voltage-dependent K^{+} channels as targets of osmosensing in guard cells. *Plant Cell* 10:1957–1970. doi:10.1105/tpc.10.11.1957
- Liu J, Raveendran M, Mushtaq R, Ji X, Yang X, Bruskiewich R, Katiyar S, Cheng S, Lafitte R, Bennett J (2003) Proteomic analysis of drought-responsiveness in rice: OsADF5. In: Tuberosa R, Phillips RL, Gale M (ed) *Proceedings of the International Congress ‘In the Wake of the Double Helix: From the Green Revolution to the Gene Revolution’*, 27–31 May 2003, Bologna, Italy, pp 491–505
- Livak KJ, Schmittgen YD (2001) Analysis of relative gene expression data using Real-Time quantitative PCR and the $\Delta\Delta\text{Ct}$ method. *Methods* 25:402–408. doi:10.1006/meth.2001.1262
- Luan S (2002) Signaling drought in guard cells. *Plant Cell Environ* 25:229–237. doi:10.1046/j.1365-3040.2002.00758.x
- Maai E, Shimada S, Yamada M, Sugiyama T, Miyake H, Taniguchi M (2011) The avoidance and aggregative movements of mesophyll chloroplasts in C_4 monocots in response to blue light and abscisic acid. *J Exp Bot* 62:3213–3221. doi:10.1093/jxb/err008

- Meyer RF, Boyer JS (1972) Sensitivity of cell division and cell elongation to low water potentials in soybean hypocotyls. *Planta* 108:77–87. doi:[10.1007/BF00386508](https://doi.org/10.1007/BF00386508)
- Ouellet F, Carpentier E, Cope M, Jamie TV, Monroy AF, Sarhan F (2001) Regulation of a wheat actin-depolymerizing factor during cold acclimation. *Plant Physiol* 125:360–368. doi:[10.1104/pp.125.1.360](https://doi.org/10.1104/pp.125.1.360)
- Qian G, Han Z, Zhao T, Deng G, Pan Z, Yu M (2007) Genotypic variability in sequence and expression of *HVA1* gene in Tibetan hulless barley, *Hordeum vulgare* ssp. *vulgare*, associated with resistance to water deficit. *Aust J Agric Res* 58:425–431. doi:[10.1071/AR06300](https://doi.org/10.1071/AR06300)
- Rapacz M, Kościelniak J, Jurczyk B, Adamska A, Wójcik M (2010) Different patterns of physiological and molecular response to drought in seedlings of malt- and feed-type barleys (*Hordeum vulgare*). *J Agron Crop Sci* 196:9–19. doi:[10.1111/j.1439-037X.2009.00389.x](https://doi.org/10.1111/j.1439-037X.2009.00389.x)
- Rapacz M, Stępień A, Skorupa K (2012) Internal standards for quantitative RT-PCR studies of gene expression under drought treatment in barley (*Hordeum vulgare* L.): the effects of developmental stage and leaf age. *Acta Physiol Plant* 34:1723–1733. doi:[10.1007/s11738-012-0967-1](https://doi.org/10.1007/s11738-012-0967-1)
- Rizhsky L, Liang H, Mittler R (2002) The combined effect of drought stress and heat shock on gene expression in tobacco. *Plant Physiol* 30:1143–1151. doi:[10.1104/pp.006858](https://doi.org/10.1104/pp.006858)
- Rosenmund C, Westbrook GL (1993) Calcium-induced actin depolymerization reduces NMDA channel activity. *Neuron* 10:805–814. doi:[10.1016/0896-6273\(93\)90197-Y](https://doi.org/10.1016/0896-6273(93)90197-Y)
- Schmidt von Braun S, Schleiff E (2008) The chloroplast outer membrane protein CHUP1 interacts with actin and profiling. *Planta* 227:1151–1159. doi:[10.1007/s00425-007-0688-7](https://doi.org/10.1007/s00425-007-0688-7)
- Shinozaki K, Yamaguchi-Shinozaki K (2007) Gene networks involved in drought stress response and tolerance. *J Exp Bot* 58:221–227. doi:[10.1093/jxb/erl164](https://doi.org/10.1093/jxb/erl164)
- Shinozaki K, Yamaguchi-Shinozaki K, Seki M (2003) Regulatory network of gene expression in the drought and cold stress responses. *Curr Opin Plant Biol* 6:410–417. doi:[10.1016/S1369-5266\(03\)00092-X](https://doi.org/10.1016/S1369-5266(03)00092-X)
- Sivamani E, Bahieldin A, Wraith JM, Al-Niemi T, Dyer WE, Ho T-HD, Qu R (2000) Improved biomass productivity and water use efficiency under water deficit conditions in transgenic wheat constitutively expressing the barley *HVA1* gene. *Plant Sci* 155:1–9. doi:[10.1016/S0168-9452\(99\)00247-2](https://doi.org/10.1016/S0168-9452(99)00247-2)
- Staiger CJ (2000) Signaling to the actin cytoskeleton in plants. *Annu Rev Plant Phys* 51:257–288. doi:[10.1146/annurev.arplant.51.1.257](https://doi.org/10.1146/annurev.arplant.51.1.257)
- Staiger CJ, Schliwa M (1987) Actin localization and function in higher plants. *Protoplasma* 141:1–12. doi:[10.1007/BF01276783](https://doi.org/10.1007/BF01276783)
- Tsuboi H, Wada M (2011) Chloroplasts can move in any direction to avoid strong light. *J Plant Res* 124:201–210. doi:[10.1007/s10265-010-0364-z](https://doi.org/10.1007/s10265-010-0364-z)
- Wasteneys GO, Galway ME (2003) Remodeling the cytoskeleton for growth and form: an overview with some new views. *Annu Rev Plant Biol* 54:691–722. doi:[10.1146/annurev.arplant.54.031902.134818](https://doi.org/10.1146/annurev.arplant.54.031902.134818)
- Wasteneys GO, Yang Z (2004) The cytoskeleton becomes multidisciplinary. *Plant Physiol* 136(4):3853–3854. doi:[10.1104/pp.104.900130](https://doi.org/10.1104/pp.104.900130)
- Wójcik-Jagła M, Rapacz M, Barcik W, Janowiak F (2012) Differential regulation of barley (*Hordeum distichon*) *HVA1* and *SRG6* transcript accumulation during the induction of soil and leaf water deficit. *Acta Physiol Plant* 34:2069–2078. doi:[10.1007/s11738-012-1004-0](https://doi.org/10.1007/s11738-012-1004-0)
- Yamashita H, Sato Y, Kanegae T, Agawa T, Wada M, Kadota A (2011) Chloroplast actin filaments organize meshwork on the photorelocated chloroplasts in the moss *Physcomitrella patens*. *Planta* 233:357–368. doi:[10.1007/s00425-010-1299-2](https://doi.org/10.1007/s00425-010-1299-2)
- Yang L, Zheng BS, Mao CZ, Yi KK, Liu FY, Wu YR, Tao QN, Wu P (2003) cDNA-AFLP analysis of inducible gene expression in rice seminal root tips under a water deficit. *Gene* 314:141–148. doi:[10.1016/S0378-1119\(03\)00713-3](https://doi.org/10.1016/S0378-1119(03)00713-3)
- Yoshimura K, Masuda A, Kuwano M, Kokota A, Akashi K (2008) Programmed proteome response for drought avoidance/tolerance in the root of a C₃ xerophyte (wild watermelon) under water deficits. *Plant Cell Physiol* 49(2):226–241. doi:[10.1093/pcp/pcm180](https://doi.org/10.1093/pcp/pcm180)